Technical Progress Report

Annual Report

Reporting Period: April 1, 2002 – March 31, 2003

Dr. Paul D. Ronney, Principal investigator

Report issued September 12, 2003

DOE Award # DE-FC26-02NT41336

University of Southern California
Department of Aerospace and Mechanical Engineering
Olin Hall of Engineering 430
Los Angeles, CA 90089

Disclaimer

Abstract

An ignition source was constructed that is capable of producing a pulsed corona discharge for the purpose of igniting mixtures in a test chamber. This corona generator is adaptable for use as the ignition source for one cylinder on a test engine. The first tests were performed in a cylindrical shaped chamber to study the characteristics of the corona and analyze various electrode geometries. Next a test chamber was constructed that closely represented the dimensions of the combustion chamber of the test engine at USC. Combustion tests were performed in this chamber and various electrode diameters and geometries were tested.

The data acquisition and control system hardware for the USC engine lab was updated with new equipment. New software was also developed to perform the engine control and data acquisition functions. Work is underway to design a corona electrode that will fit in the new test engine and be capable igniting the mixture in one cylinder at first and eventually in all four cylinders. A test engine was purchased for the project that has two spark plug ports per cylinder. With this configuration it will be possible to switch between corona ignition and conventional spark plug ignition without making any mechanical modifications.

Table of Contents

Experimental Apparatus

A. Corona Generator and Cylindrical Test Chamber

The experimental set up consists of an electronic system to generate pulsed corona discharges and a combustion cylinder with measurement and gas handling system (Fig. 1). The pulsed power includes a high voltage pulse generator utilizing a thyratron (Triton F-211) and a Blumlein transmission line to create a high voltage pulse (typ. 30-55 kV) with narrow pulse width (typ. 150 nsec). The repetition rate was 1Hz and maximum pulse energy employed was 1.8 J. All the signals were displayed and recorded by a digital oscilloscope (Tektronix TDS 420A).

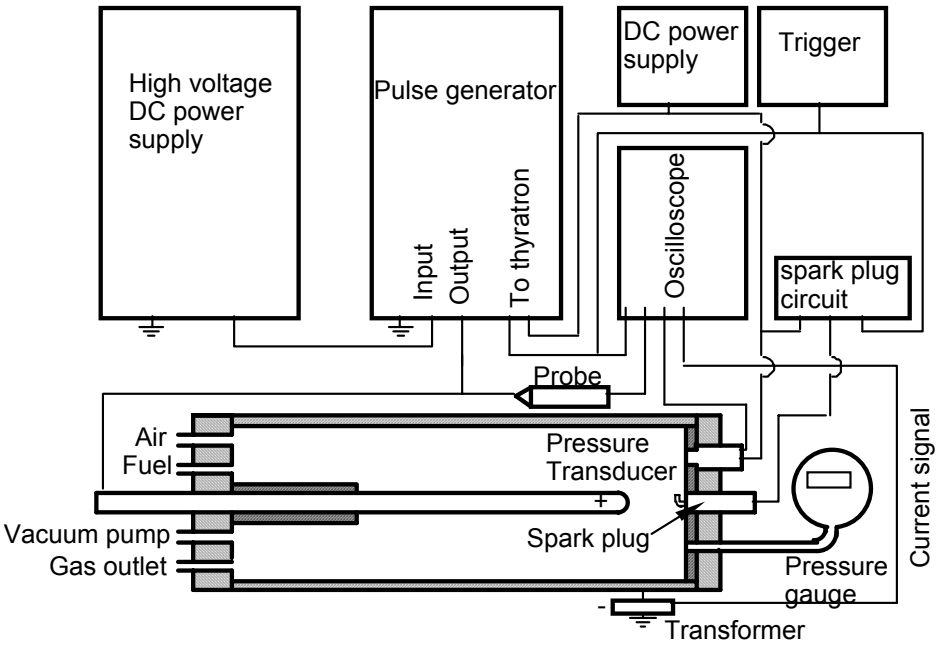

Figure 1. Experiment setup for investigation of flame ignition by pulsed corona discharge

The combustion cylinder is shown in Fig. 2. A stainless steel tube was used as an outer electrode (2.5" ID) and an interchangeable metal rod placed at its central axis as another (central) electrode. The outer electrode is always grounded and the central electrode is connected to high voltage. In this report all reported experiments were done with positive corona (central electrode is anode) unless otherwise noted.

There are gas inlets, outlet and vacuum pump inlet in one end plate and pressure gauge (Omega, DPG1000B), pressure transducer (Omega PX4201) and conventional car sparkplug (Bosch, platinum) on the other end plate. The sparkplug was switched by a standard car ignition circuit (GM Chevy Citation 81). In some cases a homemade spark plug with 1mm spacing between electrodes was used. A transparent plastic end plate was used for end view photos.

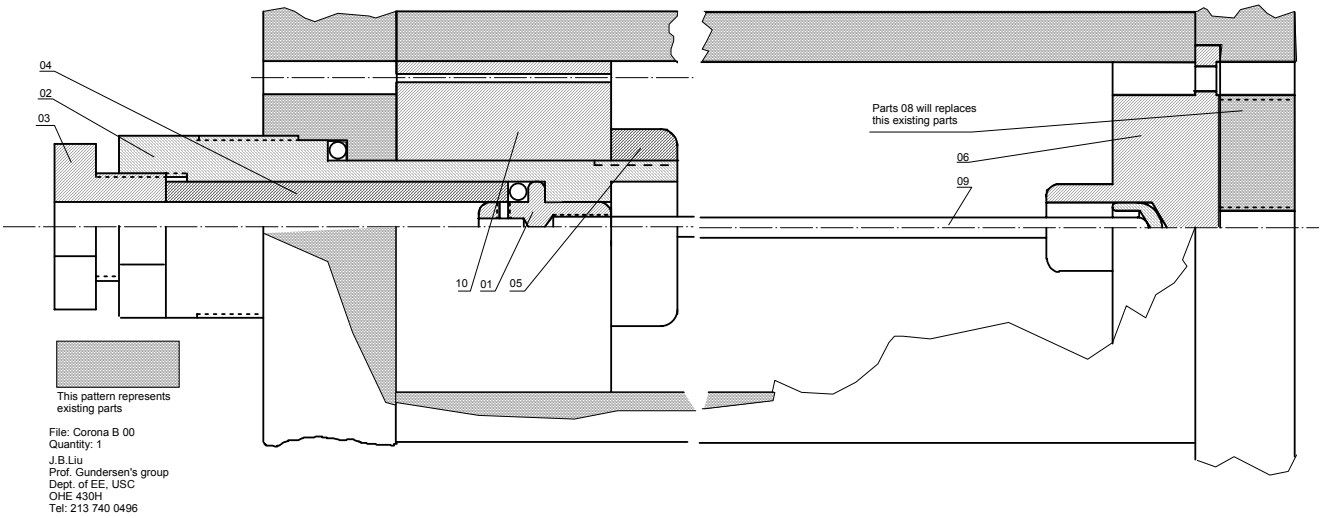

Figure 2. Cutaway drawing of test chamber

B. Engine Cylinder Test Chamber

The second test chamber used for the corona ignition experiments was modeled after the dimensions of the combustion chamber in the test engine. This chamber was constructed from 6061 T6 aluminum and consists of a bottom half that is machined into the shape of the piston dome of the test engine, and a top half that is machined to closely match the volume of the cylinder head. The two pieces are bolted together with six 5/16" bolts and are sealed with an O-ring (figs. 3 and 4). With this test chamber various electrode shapes and configurations could be tested much more quickly than in the engine. For tests performed at 1 atmosphere, the corona generator and the measurement equipment are identical to those used with the cylindrical shaped chamber. For tests run at elevated pressures a Kistler model 603B1 spark plug-mounted pressure transducer and model 5004 dual mode amplifier were used to measure the pressure. When performing ignition tests in this chamber the gas and air mixture was premixed in a larger chamber (Fig. 3). Combustion tests were performed at initial pressures up to 9 atmospheres. An alternate chamber top plate was fabricated from a ¼" plate of aluminum that leaves the sides open for photographing the test chamber (Fig. 6).

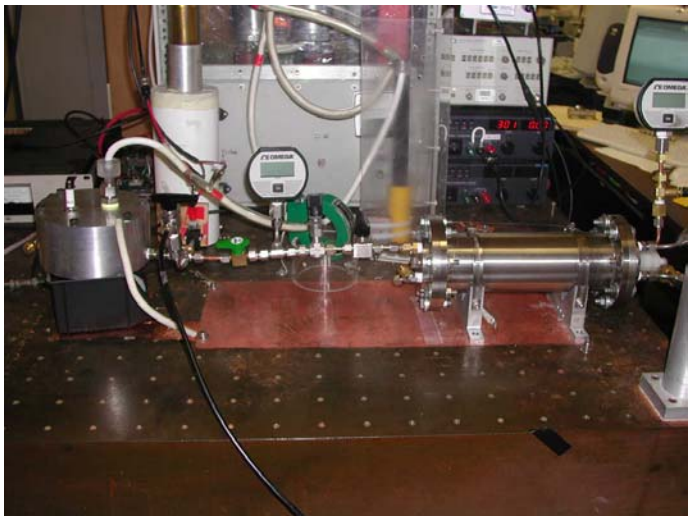

Figure 3. Experimental setup for engine cylinder test chamber

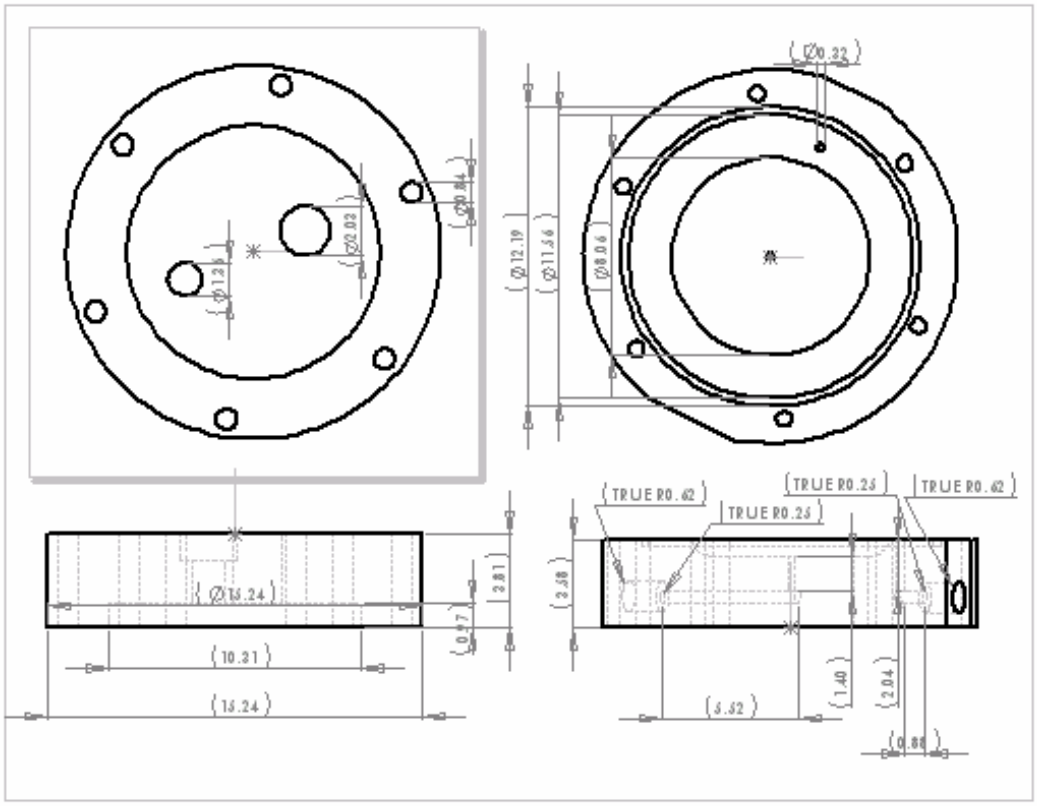

Figure 4. Dimensioned drawing of Engine Cylinder Test Chamber

Figure 5. Exploded view of Engine Cylinder Test chamber assembly, shown with circular ring electrode

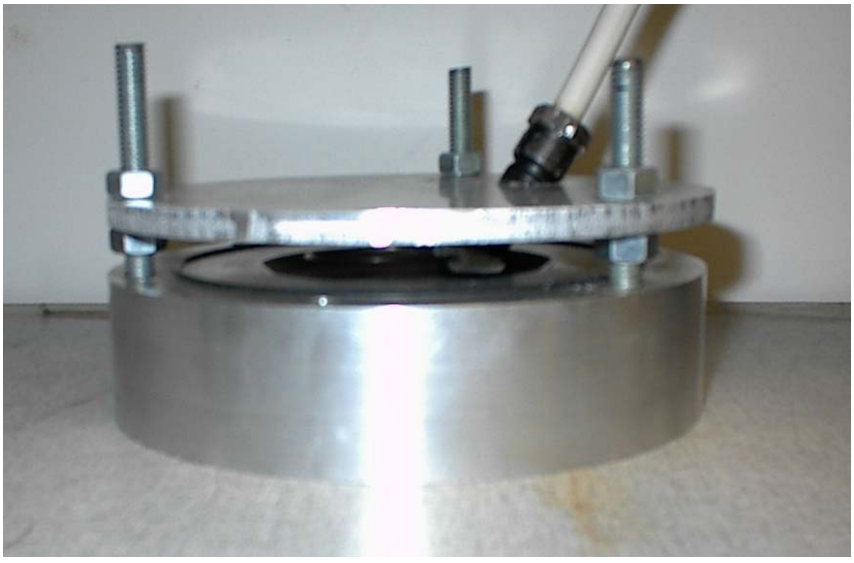

Figure 6. Engine cylinder test chamber in open configuration for visualizing corona discharge.

C. Engine, Data Acquisition and Control System

A new test engine was required to simplify the testing of the corona discharge ignition system in the engine. The engine purchased was a 2.5 liter 4 cylinder engine from a 2000 Ford Ranger Pickup. This engine was chosen because it has two spark plug ports per cylinder. This will allow the corona electrode to be inserted into one of the ports and a conventional spark plug with cylinder pressure transducer to be inserted in the other. The engine was adapted to run on natural gas using the control valve and flow meter from the previous test engine.

New data acquisition and control hardware was purchased from National Instruments for the engine lab. This was necessary as the existing data acquisition equipment was obsolete and not compatible with a modern PCI bus PC. The new equipment consists of a PCI-6031E DAQ card, a PCI-7344 motion control card, an AMUX-64T terminal block for thermocouple inputs, a SCB-68 terminal block for analog inputs, a MID-7604 stepper motor driver and a CB68-LPR terminal block for digital IO (Fig. 7).

Figure 7. Main panel for data acquisition and control equipment. Top left AMUX-64T, top right SCB-68, bottom left MID-7604, bottom right CB68-LPR

New software was developed using LabView to interface with the new hardware. The software displays all of the pertinent engine parameters and incorporates PID control for the air/fuel ratio and dyno load control. The user interface was developed to be easy to read and user friendly (Fig. 8). Warning alarms and safety shutdowns were incorporated to protect the engine when parameters (pressures, temperatures or speed) get out of a safe range.

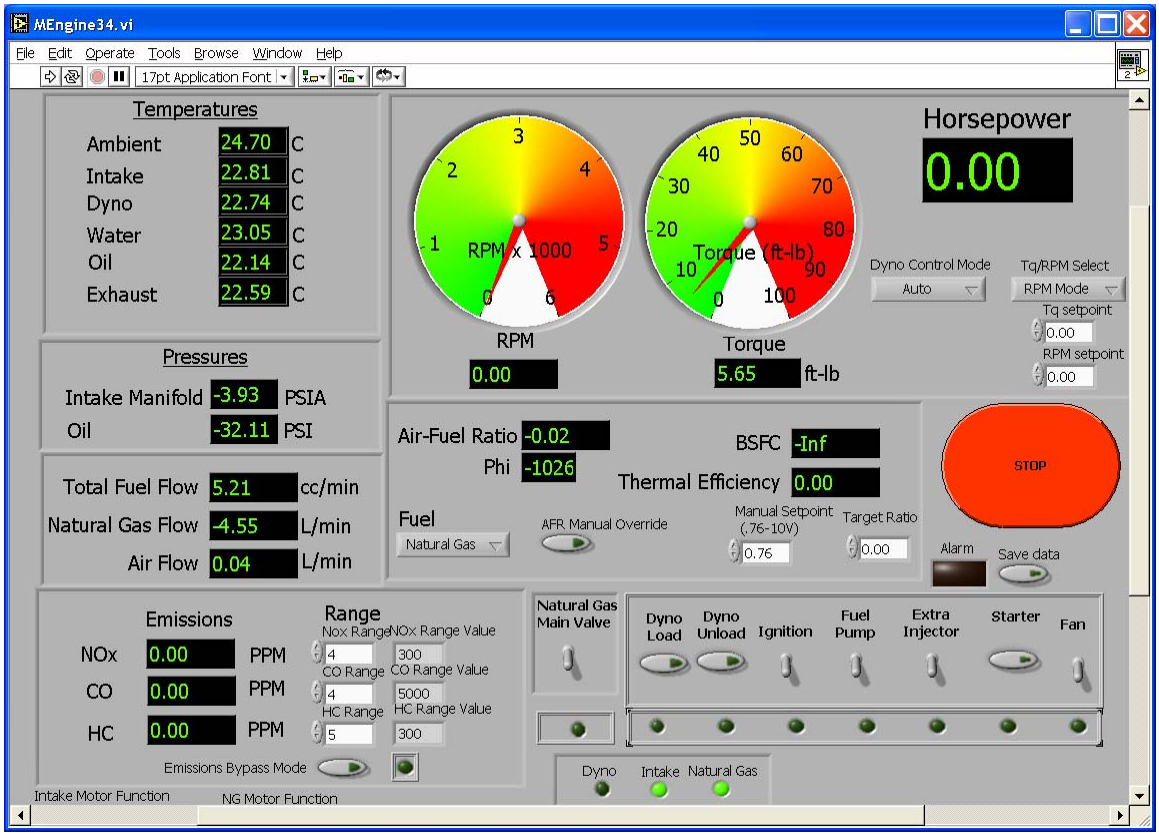

Figure 8. Screen capture of PC engine Control Panel

Results and Discussion

The experimental procedure for bench testing the corona discharge in either chamber was as follows. Evacuate the test cylinder with a vacuum pump until the pressure gauge of 1/100 psi precision shows zero reading. Then fuel (CP grade) and air (dry cylinder air) were filled into the cylinder. Composition was controlled with a digital pressure gauge with precision of 1/100 psi. After igniting with either pulsed corona or spark discharge, pressure curve was measured by the pressure transducer. Pressure signals were read and recorded by the digital oscilloscope.

A. Electrical Characteristics

Photographs of various pulsed corona discharge are shown in Figs. 9 and 10. They were taken in a completely dark environment. Fig. 9 is a pulsed corona discharge with a plain electrode viewing from the end of cylindrical chamber. This shows many streamers distributed along the length of central electrode and superimposed with each other. If viewed from side many discrete streamers evenly distributed on the surface of the central electrode are evident. The average separation between streamers is 5mm and average diameter is 0.7mm. An estimated number of streamers on the central electrode is 600. When pulse energy was reduced from 356mJ/pulse to 44mJ/pulse the total number of streamers did not change noticeably, but the brightness of streamers decreased.

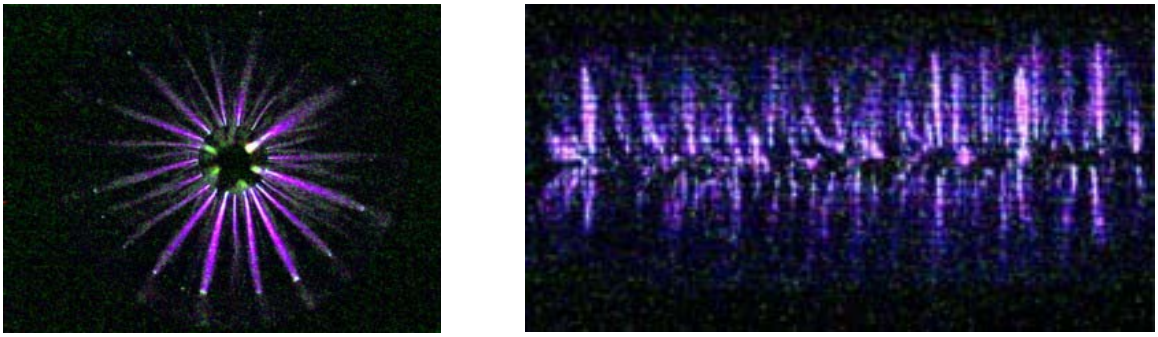

Figure 9. Left: Picture of pulsed corona discharge (end view). Diameter of central electrode: 6.35mm, Energy: 251mJ/pulse. Right: Picture of pulsed corona discharge (Side view). Diameter of central electrode: 6.35mm , Energy: 356mJ/pulse

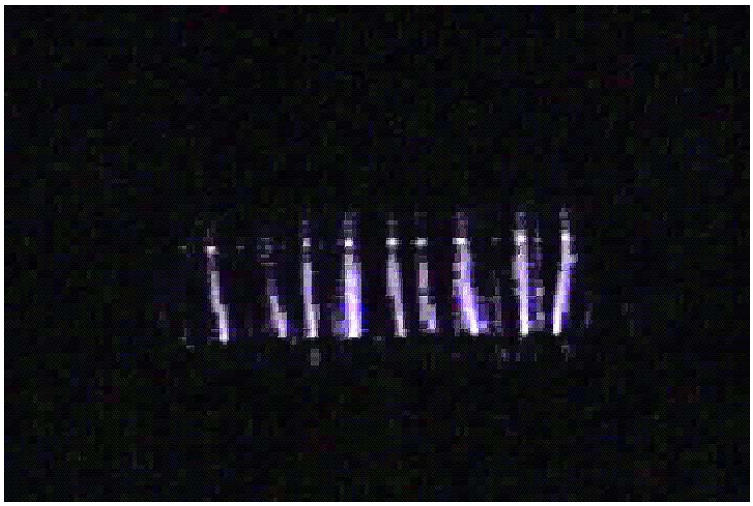

Figure 10. Photograph of corona discharge in engine cylinder test chamber with open top plate installed. .5mm diameter electrode 50mm circular ring

Figure 11 shows typical voltage, current and energy waveforms of pulsed corona discharges with (dashed curves) and without (solid curves) arcing. Current waveforms in Fig. 11b clearly show the difference between corona discharges with arcing and without arcing. Both dashed and solid curves have a first peak that corresponds to the corona discharge. Only the dash curve has the second current peak which correspondences to arc discharge. Comparing Figs. 11a,b and c, one can see that after arcing (at 150ns after trig where current started to rise rapidly) voltage drops rapidly. Consequently, no rapid energy increase was observed on energy waveform (Fig. 11c) implying that arcing does not contribute significantly to energy input to plasma at the voltages at which arc is going to start, during times ≈100's nsec. In these experiments the experimental conditions (mainly the applied voltage and electrode structure) were so controlled that no arcs were observed to ensure that only the transient phase occurred before the formation of arcing. Typical voltage pulse width (FWHM) is 140ns, and current pulse width 80ns. Figures 12 and 13 show similar results for the engine cylinder test chamber.

Pulse energy as a function of peak voltage was observed for various electrodes. The pulse energy increases non-linearly and is faster at higher peak voltages. There is an intercept peak voltage, below which no energy output to plasma, i.e. pulse corona discharge starts at a certain value of peak voltage. The intercept peak voltage decreases as decreasing of diameter of central electrode. At the same peak voltage, a thinner central electrode provides higher pulse energy than a thick central electrode does. A threaded electrode produces higher pulse energy than smooth electrode (plain electrode) with the same diameter and peak voltage. In our particular conditions, brush-like electrodes provide best electrical performance. Positive corona discharge (central electrode is anode) is much better than negative corona discharge (central electrode is cathode). In the experiments reported below, only positive pulsed corona discharge is used.

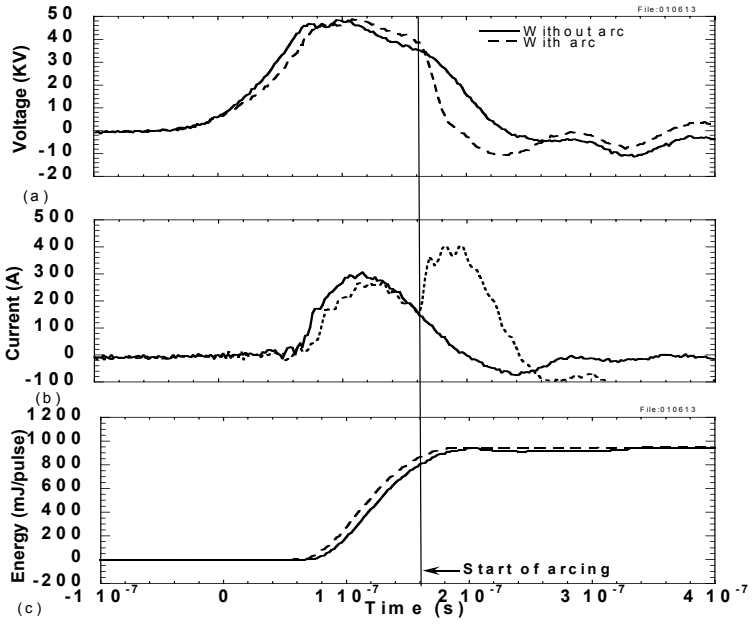

Figure 11.Voltage (a), Current (b) and Energy (c) of pulsed corona discharge with (dash curve) and without (solid curve) arc. Energy: 956mJ/pulse. Tests performed in cylindrical test chamber

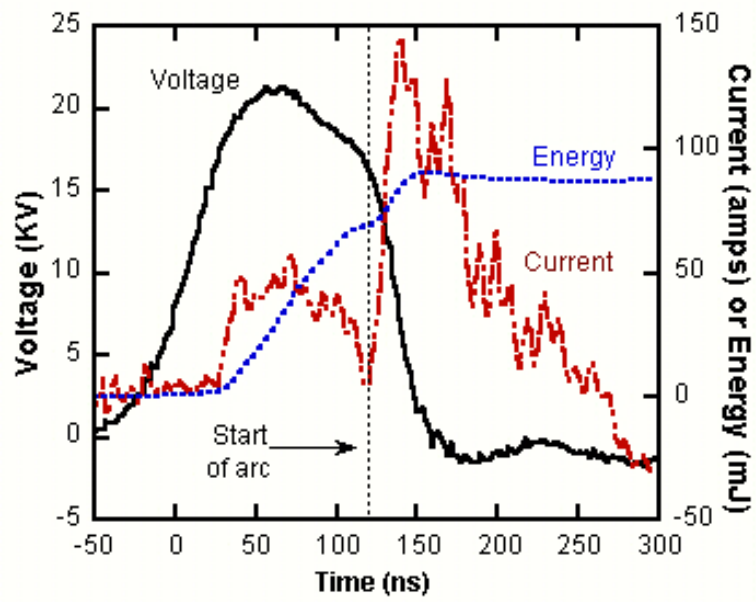

Figure 12. Plot of Voltage, Energy and Current delivered to the gas for Corona discharge plus Arc. Test performed in engine cylinder test chamber.

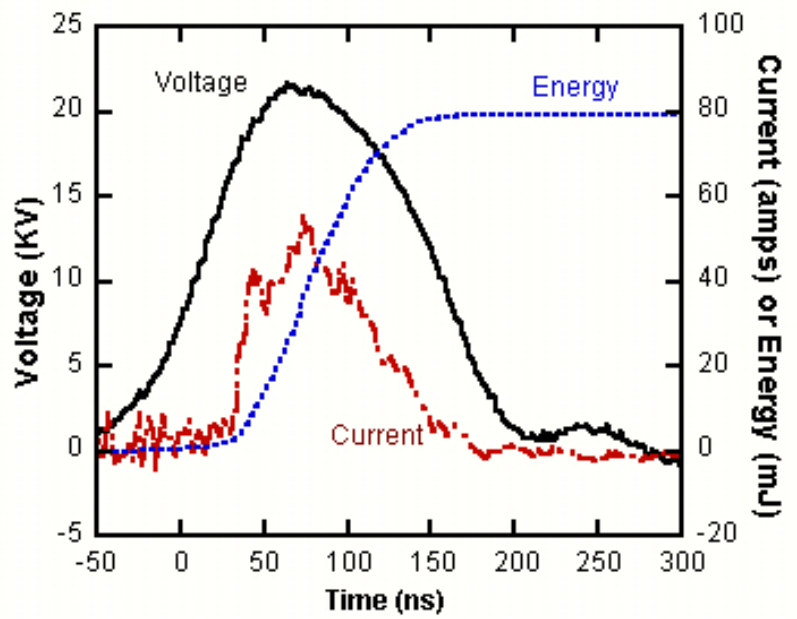

Figure 13. Plot of Voltage, Energy and Current delivered to the gas for Corona discharge only. Test performed in engine cylinder test chamber.

B. Combustion Characteristics

Figure 14 shows a typical pressure waveform. The pressure rose slowly after trigger for a period of time, then suddenly increased rapidly at a certain point, reached its maximum and finally dropped gradually. We define ignition delay time as the interval between trigger and the moment at which the pressure rises to 10% of its maximum value. Pressure rise time is defined as the interval between moments at which pressure rises to 10% and 90% of its maximum value. Peak pressure is the maximum pressure during entire process.

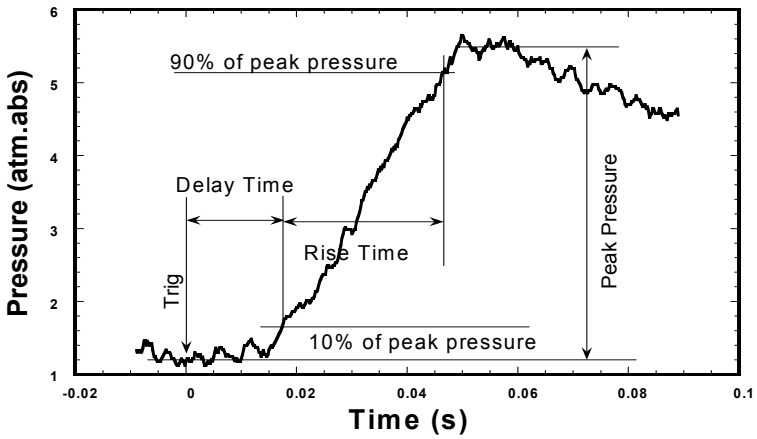

Figure 14. Typical pressure waveform with definitions of ignition delay time, pressure rise time and peak pressure.

Figure 15 shows the pressure rise time as a function of corona pulse energy for various equivalence ratios. For each equivalence ratio there is an energy value (e.g. ~300mJ/pulse for equivalence ratio 1.0), below which the pressure rise time decreases rapidly as pulse energy increases, and above which the pressure rise time is approximately constant. This behavior shows that pulsed corona discharge does affect flame ignition, and there is an "optimal energy", pulse energy higher than optimal energy is not necessary for ignition improvement. This optimal energy increases as equivalence ratio decreases. Similar tendencies are found in curves of ignition delay time (Fig. 16) and peak pressure versus corona pulse energy. When the pulse energy is smaller than optimal energy, ignition delay time decreases and peak pressure increases as pulse energy increases. When pulse energy is larger than optimal energy, all these parameters are approximately constant as pulse energy varies.

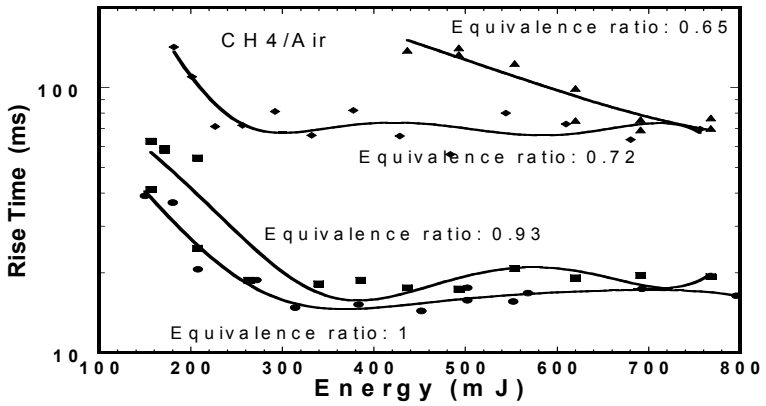

Figure 15. Pressure rise time versus pulse energy for various equivalence ratios.

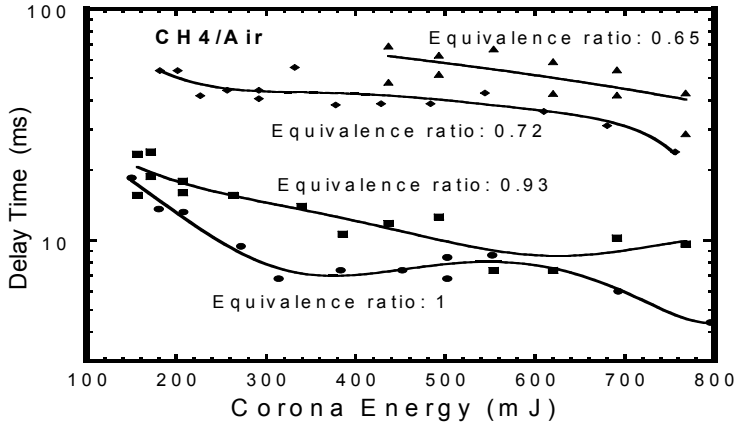

Figure 16. Ignition delay time versus pulse energy for various equivalence ratios.

Three different electrode geometries were tested in the engine cylinder test chamber, a ring shaped electrode, a straight electrode and a single pin point electrode. The ring electrode allowed the most electrical energy to be deposited to the gas before arcing so it was used for the corona combustion tests. Due to the smaller chamber size of the engine cylinder test chamber the center electrode is much closer to the chamber walls than in the larger cylindrical test chamber and is more likely to arc. Arcing usually occurs at the tip

of the electrode or at a sharp bend. In order to prevent the electrode from arcing the end of the electrode was insulated. Without this insulation the energy of the corona was too low to ignite the air/fuel mixture in the cylinder. Figure 17 shows the pressure rise time in the engine cylinder test chamber for corona only ignition, corona plus arc and for a conventional spark plug. It can be seen that the corona ignition delivers a steeper pressure rise than the conventional spark plug and a higher peak pressure. When the power was increased to allow the corona to arc the peak pressure was higher than the corona alone but it comes at the expense of additional electrical energy needed to produce the arc.

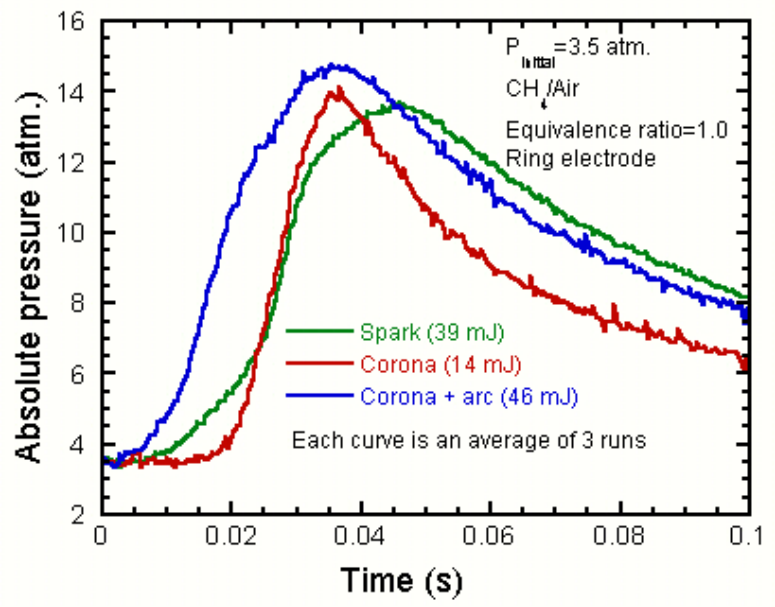

Figure 17. Plot of Pressure vs. Time for Corona, Corona + arc and conventional spark plug with associated electrical energy. Tests performed in engine cylinder test chamber.

Figures 18-20 show the dependence of ignition delay time, pressure rise time and peak pressure on equivalence ratio for iso-octane/air mixtures ignited by pulsed corona discharge as well as by spark discharge at pressures of 1.0 and 0.6 atm. Since the combustion properties of flame ignited by spark discharges are dependent on the location of the igniter, different locations of spark plug were tested and the optimum location is at center of the test cylinder. In the text below, whenever comparison is made between pulsed corona and spark discharge ignition with spark ignition at the center of the test cylinder.

As shown in Figs. 18-20, in the equivalence ratio range of 0.8 to 1.4 and initial pressure of 0.6 and 1.0 atm., C_8H_{18}/Air flames ignited by pulsed corona discharge have similar tendencies to flames ignited by spark discharges, but shorter ignition delay time, shorter (by a factor of 2) pressure rise time and higher peak pressure than spark-ignited discharges. Experiments with methane, propane, isobutene, n-butane and iso-octane show similar behavior.

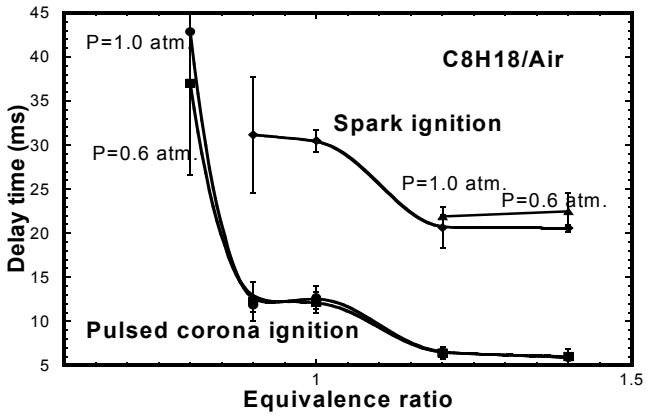

Figure 18. Ignition delay time versus equivalence ratio of C_8H_{18}/Air flames: Comparison between pulsed corona and spark ignition. Corona discharge energy: 1521mJ (1 atm.) 1509mJ (0.6atm.). Spark Energy: 70mJ (1 atm.) 68mJ (0.6 atm.).

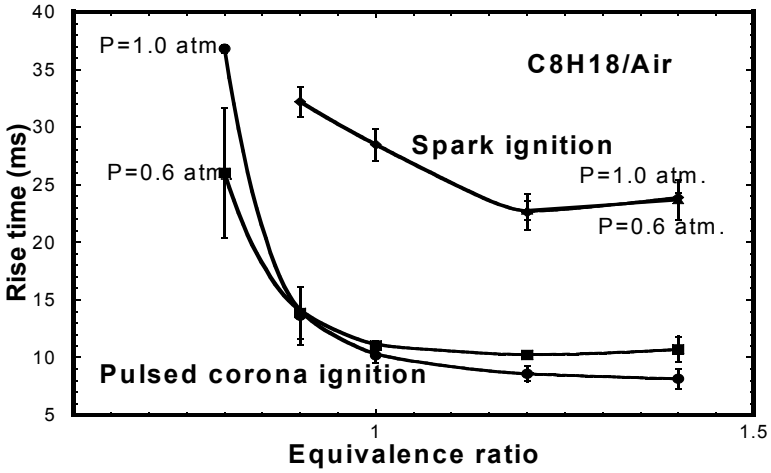

Figure 19. Pressure rise times versus equivalence ratio of C_8H_{18}/Air flame. Comparison between pulsed corona and spark discharge ignition. Energy same as Fig. 18.

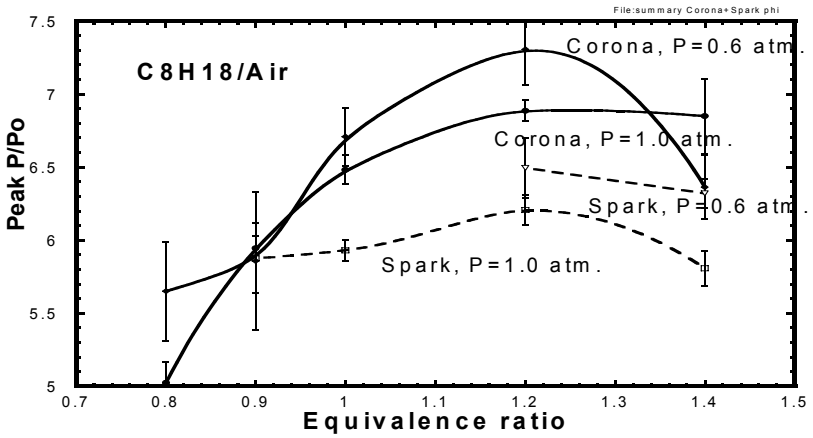

Figure 20. Peak pressure versus equivalence ratio of C_8H_{18}/Air flame. Comparison between corona and spark ignition. Energy same as Fig. 18.

Conclusion

An advantage of the pulsed corona discharge ignition occurs as the result of the creation of several hundred spatially distributed discharges. This is produced by the transient high field condition, and cannot occur for an extended time, thus is a result of the different characteristics (the complex electron energy distribution and concomitant collisional electron excitation processes). (Fig. 9) This fills a large portion of the test cylinder as compared to the single discharge channel for conventional spark discharges. Depending on how many discharge channels have enough energy to ignite flames, this multi-site ignition mechanism significantly reduces the times necessary for chemical reaction propagation, resulting shorter ignition delay and pressure rise times. Chemical advantages of corona discharges are related to the higher initial concentration of radicals created by the higher electron energy of the pulsed corona process. Computations [20, 21] show that radical ignition sources exhibit about half the ignition delay (defined as time difference between energy deposition and virtual time origin of the steadily propagating flame) of thermal ignition sources having the same energy input (though minimum ignition energies are similar for radical and thermal sources).

To study the roles of these two factors, rise times were measured for three different discharge cases (Fig. 19). The first is pulsed corona with a threaded electrode, which is a typical pulsed corona discharge and has discharge along entire length of electrode. The second is the pulsed corona with single needle electrode at the center of the test cylinder. In this case the transient discharge concentrates on the tip of the needle. The third is conventional spark discharge at center of test cylinder. The results in Fig. 19 show that spark discharge results is close to that of pulsed corona discharge with single needle electrode but far from that of pulsed corona discharge with threaded electrode. That implies that the discharge distributed along the length of the central electrode plays a major role. A more detailed investigation of the initiation of different chemical processes is underway.

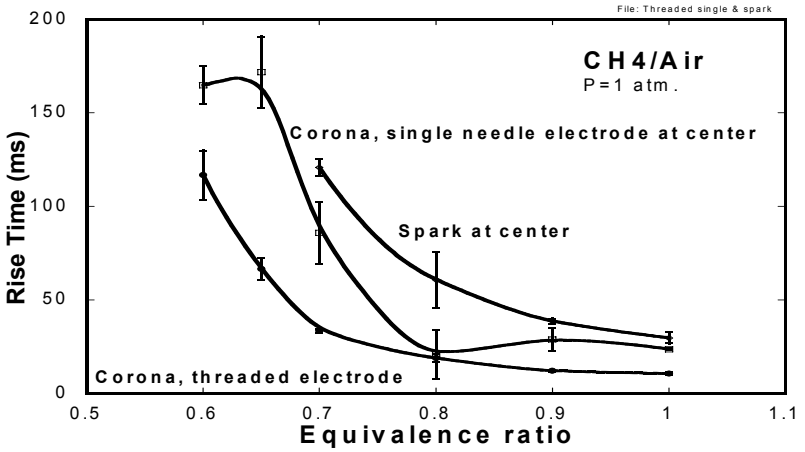

Figure 19. Comparison of rise times between spark ignition, corona ignition with single needle electrode and corona ignition with threaded electrode. Energy: 710 mJ (threaded electrode), 410 mJ (Single needle electrode) and 70 mJ (spark).

As mentioned previously, Fig. 15 suggests that there exist an optimal pulse energy, below which all the combustion parameters investigated are noticeably dependent on pulse energy, above which they are approximately constant. That could be explained as follows. As stated in section 2a, the number of channels of pulsed corona discharge is relatively independent of pulse energy. A "minimum streamer energy" (or perhaps minimum energy per unit length of streamer) for ignition probably exists, analogous minimum ignition energies for conventional spark discharges. At low pulse energies only a fraction of these discharge channels contain enough energy to initiate successfully flame kernels. With increasing pulse energy, more channels can initiate kernels, causing shorter ignition delay and pressure rise times. Above some pulse energy (optimum pulse energy), most channels can initiate kernels, thus further pulse energy increases have little effect on ignition delay and pressure rise times.

These results suggest pulsed corona discharges yield shorter ignition delay and pressure rise times by creating more extensive spatially distributed ignition sites within the combustible gas mixture. For our discharge generator and geometry, the number of streamers seems to be independent of pulse energy. Ignition delay and pressure rise times are determined primarily by the fraction of streamers containing sufficient energy for ignition. For conditions requiring high minimum streamer energy (e.g. low equivalence ratio) or in cases where rising of pulse energy is limited by arcing, fewer kernels will successfully ignite flame kernels, thus ignition delay and pressure rise times will be longer even approach those of spark discharges (note ignition delay and pressure rise times of pulsed corona discharge ignition approach but rarely exceed those of spark discharges.). Presumably minimum streamer energies follow the same trends as minimum ignition energies for spark discharges, higher for very lean or rich mixtures [21], lower pressures [21], and higher Lewis numbers [22].

The experimental results of pulsed corona discharge ignition described above are preliminary, but show some features that conventional spark discharge does not have. Spatially extensive multi-site ignition, faster ignition and pressure delay times (typically a factor of 3) and higher peak pressure along with possibility of NO_x removal is of interest and will be investigated and may provide new possibilities for advanced combustion techniques as well as new field for fundamental combustion research. The next phase of testing will take what has been learned from the bench tests and implement a corona electrode as the ignition source for one cylinder of the test engine.

References

[1] J.B.Heywood. Internal combustion engine fundamentals, McGraw-Hill, New York, 1988.

[2]. J. D. Dale, P. R. Smy, and R. M. Clements, "Laser Ignited Internal Combustion Engine - An Experimental Study," *SAE Paper No. 780329* (1978.)

[3] Kailasanath, K., "Review of propulsion applications of detonation waves," *AIAA J.*, Vol. 38, pp. 1698-1708 (2000); Kailasanath, K., "A review of PDE research - performance estimates," AIAA Paper 2001-0474 (2001).

[4] Schauer, F., Stutrud, J., Bradley, R., "Detonation initiation studies and performance results from pulsed detonation engine applications," AIAA Paper No. 2001-1129 (2001).

[5] Bussing, T. R. A., Bratkovich, T. E., and Hinkey, J. B., "Practical Implementation of Pulse Detonation Engines," AIAA Paper 97-2748, July 1997.

[6] Cote, T., Ridley, J.D. Clements, R.M. Smy, P.R., "The ignition characteristics of igniters at sub-atmospheric pressure", Combust. Sci. and Tech. Vol.48, pp 151-162, 1986.

[7] D. Yossefi, S.J. Maskell, S.J. Ashcroft and M.R. Belmont,"Ignition source characteristics for naturel-gas-buring vehicle engines", Proc Instn. Mech Engrs Vol 214 Part D 171-180,2000

[8] M. Lavid, A.T. poulos, S.K. Gulati, Y. Nachshon and J.G. Stevens, "Excimer laser relight for the supersonic commercial transport aircraft" SPIE Vol. 1862 , 59-70 (1993)

[9] R. Maly, "Spark ignition: Its physics and effect on the internal combustion engine" in "Fuel Economy in road vehicles powered by spark ignition engines" ed. J.C. Hilliard and G.S.Springer, Plenum Press, New York , 1984, 91-148

[10] R. Maly and M. Vogel, "Initiation and propagation of flame fronts in lean CH4-air mixtures by the three modes of the ignition spark" Seventeenth Symposium (International) on Combustion 821-831, The Combustion Institute, 1978

[11] R. Maly," Ignition model for spark discharge and the early phase of flame front growth" Eighteenth Symposium (International) on Combustion 1747-1753, The Combustion Institute, 1981

[12] E.M. Bazelyan and Yu.P. Raizer, "Spark Discharge", CRC Press, Boca Raton, New York, 1998.

[13] Y.L.M. Creyghton, "Pulsed positive corona discharges", Thesis Eindhoven, 1994.

[14] Roth, G.J., and Gundersen, M.A., "Laser induced fluorescence of NO distribution after needle-plane pulsed negative corona discharge, IEEE transactions on plasma science, Vol. 27,No. 1 28-29

[15] Puchkarev, V., Roth, G., and Gundersen, M, "Plasma processing of diesel exhaust by pulsed corona discharge", International fall fuels and lubricants meeting and exposition, San Francisco, California, Oct. 19-22,1998, SAE technical paper series 982516

[16] These results have been reported at AFOSR and ONR contractors meetings. Additional details are provided at: http://carambola.usc.edu.

[17] Civitano, L., "Industral application of pulsed corona processing to flue gas",in " Non-Thermal plasma techniques for pollution control" ed. Penetrante, B.M. and Schultheis, S.E., Springer-Verlag Berlin Heidelbers, 1993, 0.3-130.

[18] M. Goldman and A. Goldman, "Corona discharge" in "Gaseous Electronics" ed. M.N. Hirsh and H.I. Oskam, 219-291.

[19]Y.L.M. Creyghton. E.M. van Veldhuizen and W.R. Rutgers, Electrical and optical study of pulsed positive corona, in Non-Thermal Plasma Techniques for pollution control edited by B.M. Penetrante and S. Schultheis, Springer-Verlag Berlin Heidelberg, 1993

[20]. Dixon-Lewis, G., Shepard, I.G., *Proc. Combust. Inst.* 15:1483-1491 (1974).

[21]. T. M. Sloane, *Combust. Sci. Tech.* 73:351-365, 1990.

[22]. Lewis, B., von Elbe, G., *Combustion, Flames, and Explosions of Gases*, 3rd Ed., Academic Press, 1987.

[23] JianBang Liu, Paul D. Ronney, Fei Wang, L.C. Lee and Martin Gundersen, "Transient plasma ignition for lean burn applications" 41st Aerospace Sciences Meeting, 5th Weakly Ionized Gases Workshop, Reno, Nevada 6 - 9 Jan 2003

[24] Martin A. Gundersen, Andras Kuthi and Jianbang Liu, "Transient plasma ignition physics for pulse detonation engines" 15th ONR propulsion meeting, Washington, DC, August 5-7, 2002